Science of the Total Environment 728 (2020) 138611

Contents lists available at ScienceDirect

Science of the Total Environment

journal homepage: www.elsevier.com/locate/scitotenv

In vitro intestinal toxicity of commercially available spray disinfectant products advertised to contain colloidal silver

Kim R. Rogers [a,*], Taylor E. Henson [b,c], Jana Navratilova [a], Mark Surette [a], Michael F. Hughes [c], Karen D. Bradham [a], Aleksandr B. Stefaniak [d], Alycia K. Knepp [d], Lauren Bowers [d]

[a] Watershed and Ecosystem Characterization Division, Center for Environmental Measurement and Modeling, Office of Research and Development, USEPA, RTP, NC 27711, United States
[b] Oak Ridge Institute for Science and Education, Research Triangle Park, NC 27711, United States
[c] Chemical Characterization and Exposure Division, Center for Computational Toxicology and Exposure, Office of Research and Development, USEPA, RTP, NC 27711, United States
[d] National Institute for Occupational Safety and Health, Morgantown, WV 26506, United States

HIGHLIGHTS

- Physicochemical properties and cytotoxicity were determined for colloidal silver spray products.
- Products showed a high degree of variability for claimed vs. measured total silver.
- Cytotoxicity was measured using a rat intestinal epithelial cell (IEC-6) model.
- Cell viability was affected by each of the consumer products.
- Cytotoxicity was attributed to the particulate silver, soluble silver or non-silver matrix constituents.

GRAPHICAL ABSTRACT

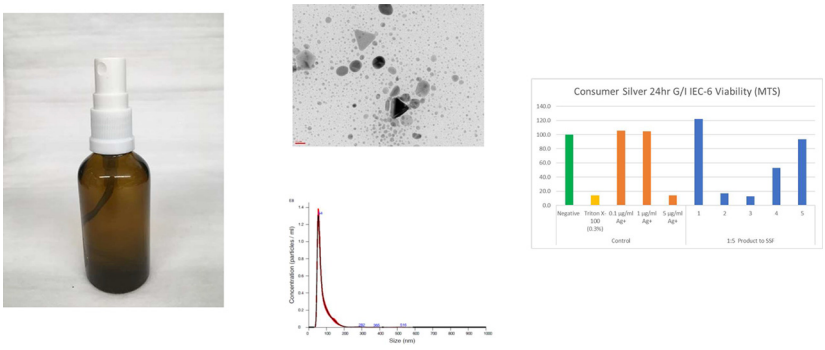

ARTICLE INFO

Article history:
Received 19 February 2020
Received in revised form 8 April 2020
Accepted 8 April 2020
Available online 14 April 2020

Editor: Damia Barcelo

Keywords:
Colloidal silver
Bioavailability
Silver nanoparticles

ABSTRACT

The use of colloidal silver-containing products as dietary supplements, immune boosters and surface disinfectants has increased in recent years which has elevated the potential for human exposure to silver nanoparticles and ions. Product mislabeling and long-term use of these products may put consumers at risk for adverse health outcomes including argyria. This study assessed several physical and chemical characteristics of five commercial products as well as their cytotoxicity using a rat intestinal epithelial cell (IEC-6) model. Concentrations of silver were determined for both the soluble and particulate fractions of the products. Primary particle size distribution and elemental composition were determined by transmission electron microscopy (TEM) and energy-dispersive X-ray spectroscopy (EDS), respectively. Hydrodynamic diameters were measured using nanoparticle tracking analysis (NTA) and dynamic light scattering (DLS). The effect of gastrointestinal (GI) simulation on the colloidal silver products was determined using two systems. First, physical and chemical changes of the silver nanoparticles in these products was assessed after exposure to Synthetic Stomach Fluid (SSF) resulting in particle agglomeration, and the appearance of AgCl on the surfaces and between particles. IEC-6 cells were exposed for 24 h to dilutions of the products and assessed for cell viability. The products were also treated with a three-stage simulated GI system (stomach and intestinal fluids) prior to exposure of the IEC-6 cells to the isolated silver nanoparticles. Cell viability was affected by each of the consumer products. Based on the silver nitrate and commercial silver

* Corresponding author at: 109 T.W. Alexander Drive, U.S. EPA, Research Triangle Park, NC 27709, United States.
E-mail address: rogers.kim@epa.gov (K.R. Rogers).

https://doi.org/10.1016/j.scitotenv.2020.138611
0048-9697/Published by Elsevier B.V.

nanoparticle dose response, the cytotoxicity for each of the colloidal silver products was attributed to the particulate silver, soluble silver or non-silver matrix constituents.

Published by Elsevier B.V.

1. Introduction

Due to its antimicrobial activity, colloidal silver (colloidal being defined as suspensions containing particles between 1 nm and 1 μm) has a long history of use for medical applications. As a result of the introduction of effective antibiotics in the 1940s, most uses of colloidal silver by the medical profession, except for some topical uses, were abandoned except for topical silver used for bandages to treat burns. Nevertheless, in the past several decades, there has been a resurgence of colloidal silver products advertised to the general public for various applications including dietary supplements, immune boosters, skin disinfectants and surface disinfectant sprays. These products are readily available online and through specialty health product stores. Sales and use of these products continue to increase despite health risk warnings from reputable medical organizations (Mayo Clinic).

The US Food and Drug Administration (FDA) has indicated that "colloidal silver is not safe or effective for treating any disease or condition" (FDA, 1999). As a result, many of the colloidal silver products include statements indicating that they are not intended to treat or cure any disease. In addition, the Mayo Clinic website (Mayo Clinic) asserts that "colloidal silver is not considered safe or effective for any health claims manufacturers make https://www.mayoclinic.org. Silver has no known purpose in the body. Nor is it an essential mineral, as some sellers of silver products claim". Although the short-term use (up to 14 days) of a commercial colloidal silver preparation (dosed at 480 μg/day) did not result in any significant clinical changes (Munger et al., 2014), long-term use of colloidal silver products over a 5–10 y period, even as directed, has been reported to result in argyria (blue-gray pigmentation of the skin, eyes and nail beds) (Kwon et al., 2009; Saluja et al., 2015; Kim et al., 2019).

In addition to the wide variations in total silver concentrations for many of these products (ranging from μg/l to mg/l), discrepancies between claimed and measured levels are often observed. A recent report of the characterization of 22 colloidal silver preparations indicated a high degree of variability between the total amount of silver claimed and the amount measured by ICP-MS (Rogers et al., 2018). Colloidal silver suspensions are sold in a variety of concentration ranges and often in pump spray containers. Some preparations are advertised as surface disinfectants (not intended for direct internal use), some are intended for direct ingestion, and some are advertised for both external and internal use. Instructions for internal dose also vary from a few μg/d to several hundred μg/d for adults and children (Rogers et al., 2018).

Characterization of colloidal silver in selected liquid consumer products has been reported in a range of studies. Cascio et al. (2015) characterized six colloidal silver products with respect to size distribution as well as mass and particle number concentrations using a range of analytical techniques. Five of these products contained total measured silver concentrations similar to their declared silver mass values. Reed et al. (2014) reported on the characterization of eight commercially available dietary supplement liquids containing nanoparticles of various metals including colloidal silver. They reported that each of these products decreased the number of microvilli in an *in vitro* model of human intestinal cells relative to untreated cells. Ramos et al. (2014) reported the characterization of five colloidal silver products which contained both nanoparticulate and ionic forms of silver in the low μg/l to mg/l concentration ranges. They observed a high degree of variability between the forms of the silver claimed and the total silver measured. Lim et al. (2019) reported the characterization of nanoscale silver particles in seven liquid products claiming to contain colloidal silver. The size of the silver nanoparticles (AgNP) were all under 50 nm and total silver concentrations ranged between 3.9 and 41.7 mg/l. Rogers et al. (2018) reported the characterization of 22 commercial spray products that claimed to have colloidal silver. Although silver nanoparticles were observed in all products, a high degree of variability was noted between claimed and measured values for total silver with only seven products having total silver concentrations within 20% of their nominal reported values.

Because colloidal silver may be ingested, the potentially negative effect on the intestinal mucosa and the gastrointestinal (GI) environment should be considered in any determination of bioavailability. In addition, silver nanoparticles physically and chemically transform during passage through the GI system (Walczak et al. 2012; Rogers et al., 2012). Passage of AgNP through a simulated GI tract has been described in several reports (Bohmert et al., 2014; Miethling-Graff et al., 2014; Kastner et al., 2017). Although there appear to be some variations likely due to differences in the simulated GI fluids and AgNP sizes and initial surface coatings, the consensus seems to be that particles are aggregated and transformed by the low pH stomach environment due to dissolution and formation of AgCl and silver-protein complexes with sulfur and oxygen. Walczak et al. (2012) reported the formation of chloride interparticle bridges in the stomach environment between AgNPs as well as the formation of nanoparticles containing sulfhydryl or chloride linkages. Nevertheless, they also report that AgNPs ultimately reach the intestinal system. AgCl bridges between AgNPs in the presence of low pH synthetic stomach fluid have also been reported by Rogers et al., (2012). The transformation of both size and particle agglomerate composition was dependent on initial AgNP size and coating material (Mwilu et al., 2013). Wu et al. (2018) conducted GI simulations using a colloidal silver dietary supplement. They showed that for the relatively small AgNPs (11–17 nm), passage through a GI simulation (4 h) resulted in the dissolution of 75% of the particulate fraction. The 25% remaining AgNPs were coated with a biomolecular corona.

Given the high degree of variability shown for colloidal silver products advertised for health-related applications, we investigated the transformation of colloidal silver consumer products during simulated GI passage as well as their toxicity using a rat intestinal epithelial cell (IEC-6) model. In this report, we exposed selected colloidal silver-containing products to simulated gastrointestinal fluids and characterized structural, compositional and toxicological transformations. In addition, we suggest which of the fractions (soluble silver, particulate silver or matrix components) are responsible for cellular toxicity in the in vitro cell model.

2. Methods

2.1. Materials

Five commercially available colloidal silver spray products were purchased from the internet. These products were intended for internal consumption or as surface sanitizers intended for external use.

Silver nanospheres (polyvinylpyrrolidone (PVP)-stabilized 20 nm, biopure) were obtained from nanoComposix, (San Diego, CA, USA). All other chemicals used were of reagent grade.

2.2. Total silver concentration by ICP-OES

For the determination of total silver in colloidal suspensions, 1 ml of the product was acid digested (in triplicate) with 1 ml of concentrated nitric acid (67–70% Optima™, Fisher Scientific, Inc., Pittsburgh, PA, USA) in a hot block (DigiPrep, SCP Science, Quebec, Canada) at 60 °C

for 12 h. Prior to ICP-OES analysis, all samples were diluted 10 fold or greater (depending on the initial concentration) using distilled deionized (DDI) water (18 MΩ × cm, Millipore, Bedford, MA, USA). The analysis of the digested samples was performed using an iCAP 6500 Duo ICP-OES instrument (Thermo Scientific, Waltham,MA, USA). For quantification of silver, the spectral line at 328.0 nm was used. Scandium (spectral line 361.3 nm) was used as an internal standard. Commercially available certified reference standards (SCP Science, Quebec, Canada) were used for the preparation of calibration standards. Concentrations of chloride ions were measured by ion chromatography and sulfur was measured using ICP-MS (Table S-1).

2.3. Centrifugal ultrafiltration and estimated dissolved Ag

To estimate the dissolved silver fraction in the colloidal suspensions, centrifugal-ultrafiltration was used in which 5 ml of the product was transferred to a 10 kDa centrifuge filter unit (Amicon Ultra-15, 10 K,

Millipore, Bedford, MA, USA) and centrifuged at 5911 ×*g* for 20 min. After centrifugation, an aliquot of 1 ml of the filtrate was acid digested (in triplicate), analyzed as described above and considered to represent the proportion of silver in ionic form.

2.4. Dynamic light scattering (DLS)

DLS measurements were performed with a Malvern Zetasizer Nano ZS (Malvern, UK). 1 ml of each product was measured in single-use acrylic cuvettes (Sarstedt, Germany). The measurements were performed in triplicate at a controlled temperature of 25 °C. The intensity size distribution, the *Z*-average diameter (Z-avg), and the polydispersity index (PDI) were obtained from the autocorrelation function using the "general purpose model".

2.5. Nanoparticle tracking analysis (NTA)

NTA measurements of the consumer products were performed with a NanoSight NS500 instrument (NanoSight, UK), using a 640 nm laser. Measurements were performed at 25 °C. All samples were measured for 60 s with manual shutter and gain adjustments. The measurement settings were optimized using 100 nm polystyrene beads. The software used to capture and analyze the data was the NTA 2.3 (NanoSight Ltd.). Each video was analyzed to give a particle size distribution and an estimate of the particle concentration.

2.6. Transmission electron microscopy-energy dispersive X-ray spectroscopy (TEM-EDS)

TEM-EDS was used to verify the presence of silver nanoparticles in the colloidal suspensions and to measure their size and shape. Samples were prepared by depositing a drop of the colloidal suspension onto a carbon-coated nickel grid and allowing it to airdry overnight at room temperature. The image processing program Image J (National Institutes of Health) was used to determine the nanoparticle size distributions from TEM micrographs. Micrograph images were obtained using a FEI Titan 80–300 probe aberration corrected scanning TEM with a monochromator operating at 200 kV. A Bruker 4 SDD Energy Dispersive X-ray Spectroscopy (EDS) instrument was used to perform elemental mapping. Images were acquired at 300 kV and were representative of at least 3 grids. Image J size calculations were conducted using particle counts of 100 to 1000 particles. For the larger particles, size range values were typically determined from observations of between 10 and 20 particles.

2.7. Simulated stomach fluid (SSF) exposure

Two methods for GI simulation were used. The SSF method was used for particle characterization and the GI simulation method was used for cytotoxicity assays. Exposure of the colloidal silver suspensions to SSF is a screening method to measure particle transformation in response to low pH and high ionic strength. Gastric and intestinal proteins were excluded due to their interference with particle hydrodynamic diameter measurements. Synthetic stomach fluid (SSF) was prepared using deionized distilled (DDI) water and contained HCl (0.42 M) and glycine (0.40 M) pH 1.5 (Kelly et al., 2002). Colloidal silver suspensions were incubated (1:1 dilution in SSF) for 1 h prior to analysis of hydrodynamic diameter by NTA or DLS. For TEM-EDS the SSF-treated products were centrifuged (3000 ×*g*) for 5 min, the supernatants were removed and resulting pellets were resuspended in DDI water (using brief (5 min) sonication) to their original volume for TEM-EDS analysis.

2.7.1. Cytotoxicity assays (products and soluble fractions)

Rat small intestine epithelial cells (IEC-6) were purchased from American Type Culture Collection (ATCC®, Manassas, VA, USA). This non-transformed cell line is a two-dimensional model of the rat small intestine. The adherent cells were grown using Dulbecco's Modified Eagle Medium (DMEM) (ATCC®) with 4 mM L-glutamine, 1.5 g/l sodium bicarbonate and 4.5 g/l glucose, 10% (*v*/v) fetal bovine serum (ATCC®) and 1% by volume penicillin/streptomycin solution (100×, Corning Life Sciences, Tewksbury, MA, USA). A 0.25% solution of Gibco Trypsin-EDTA (Thermo Fisher Scientific, Waltham, MA, USA) in sterile water was used to detach cells from culture plates. IEC-6 cells were seeded in Corning CoStar clear 96-well (60,000 cells/well) tissue culture treated plates with DMEM added and placed overnight in an incubator set at 37 °C, 95% relative humidity and 5% CO_2. The following day the cells were treated with test material. Following addition of test material to the wells, the plates were returned to the incubator for 24 h.

One ml of product or filtrate was added to 4 ml of fresh culture media (37° C) to make the 1:5 dilution. These mixtures were vortexed and aliquots at 1:10 and 1:20 ratios were prepared with media for dosing of IEC-6 cells. AgNPs were sonicated (3 × 4.5 W for 3 s) into 10 ml of complete media at 1 mg/ml and aliquots of 500, 100, 50 and 10 μg/ml were made. Each sample was sonicated again just prior to dosing. Silver nitrate was dissolved in culture media at a concentration of 1 mg Ag/ml and diluted. This solution was used as a source of Ag ions. The effect of dose on cellular viability was assessed for products and filtrates at concentrations of 1:5, 1:10 and 1:20 and Ag ions at 0.1, 1, 2.5, and 5 μg Ag/ml in IEC-6 cells. The negative control was media and the positive control was 0.3% Triton X-100. IEC-6 cell viability was measured using 3-(4,5-dimethylthiazol-2-yl)-5-(3-carboxymethoxyphenyl)-2-(4-sulfophenyl)-2H-tetrazolium (MTS) (Sigma-Aldrich, St Louis, MO). After a 24-h exposure to the dilutions of products, filtrates or Ag ions, the media was removed, and the cells were washed 3 times with fresh culture media (37 °C) and replaced with 100 μl media and 20 μl MTS. The plates were returned to the incubator for 1–4 h, and then absorbance was measured at 490 nm with a SpectraMax i3 (Molecular Devices, Sunnyvale, CA, USA) plate reader.

2.7.2. Cytotoxicity assays (isolated particles after GI fluid simulation)

For cell assays, GI simulation included separate incubations with pepsin, pancreatin and intestinal bile extract (Henson et al., 2019). The particulate fraction after each incubation was collected by ultracentrifugation and sequentially incubated in each GI fluid simulants. The cells were then exposed to the treated particles after the final incubation step.

The effect of simulated gastric fluids on AgNPs within the consumer products and potential alteration on cytotoxicity was assessed. The procedure as outlined by McCracken et al. (2013) was followed. A 1 ml aliquot of each product was added to 4 ml of water with pepsin at 146 μg/ml and adjusted to pH 2 with 50 nM HCl. The sample dilutions were incubated for 1 h at 37 °C in a shaking water bath and the silver nanoparticles isolated using an ultracentrifuge. Samples were centrifuged for 1 h using a Beckman XL-80 ultracentrifuge with a 70.1Ti rotor at 60,000 rpm. The supernatant was aspirated, and the pellet was

resuspended in 5 ml of cell culture water (pH 7) with 2 mg/ml pancreatin, incubated for 1 h at 37 °C and again particles were isolated using an ultracentrifuge. The supernatant was aspirated, and the pellet was resuspended in 5 ml of cell culture water (pH 7) with 12 μg/ml intestinal bile extract incubated for 1 h at 37 °C and spun using an ultracentrifuge. After the last centrifugation step, the supernatant was again aspirated, and the pellet was resuspended in 5 ml media as described above and applied to IEC-6 cells for 24 h. Cytotoxicity was assessed with MTS as described above.

2.8. Analytical strategies and limitations for nanoparticle analysis

The separation between particulate and soluble silver was performed using centrifugal ultrafiltration membranes with a cut-off of 10 kDa. Estimates have suggested an average equivalent pore size of 3.2 nm in these membranes (Van Koetsem et al., 2017). The authors also suggested that the 10 kDa membrane will separate AgNP >14 nm from the ionic fraction. We cannot exclude the possibility that some of the very small AgNP between 3 and 14 nm passed into the filtrate fraction.

Hydrodynamic diameter measurements were made using NTA and DLS. Both techniques measure light scattered from nanoparticle suspensions and are representative of the hydrodynamic diameter for particles and particle agglomerates. These hydrodynamic diameter measurements are based on Brownian movement and are reflective of proteins, polymers or other organic molecules that may be added as stabilizers and bind to nanoparticle surfaces.

NTA is based on measurements for individual particles. Consequently, the analysis tracing represents the number count of the particle hydrodynamic diameters in each size range with the mean representing the average of the polydisperse particle size distribution. Because the particle analysis tracing shows the relative number of particles in each discrete size range (including the Mode-highest peak), it provides a representation of the particle size distribution. Nevertheless, due to light scattering limitations, AgNPs less than about 20 nm are not typically counted by this technique.

The DLS average represents the volume-weighted average size of the particle distribution. Due to the dependence of signal intensity on particle size, DLS measurements are not well suited to highly polydisperse particle suspensions. In addition, particles below 20 nm are not well accounted for in polydisperse suspensions. The polydispersity index (PDI) approaches 0.05 for highly monodisperse suspensions and values above 0.7 represent highly disperse suspensions which are not suitable for DLS analysis (Danaei et al., 2018).

The colloidal silver spray products characterized for this study varied in advertised application, concentration and appearance (color and odor). In addition to colloidal silver, these products included other ingredients such as 'essential oils, and plant extracts', hydrogen peroxide, etc. which may interact with soluble and particulate silver in unpredictable ways. These types of additives are not typically present in pristine AgNP preparations (MacCuspie et al., 2011). Consequently, our approach involved the investigation of the cytotoxic effects of soluble and particulate silver as well as product matrix effects in an in vitro rat intestinal model. GI exposure to the colloidal Ag products may occur from direct ingestion, hand-to-mouth activity and inhalation followed by mucociliary transport of the particulates from the lungs to GI tract.

3. Results and discussion

3.1. Total silver detection

The total silver concentrations for the measured products varied widely from 6.0 to 960.8 mg/l (Table 1). For product 1 the silver was primarily soluble. For Products 2, 3, 4 and 5 the measured silver was primarily particulate. The total silver concentrations for products 1 and 2 deviated widely between the claimed and measured values. Products 3, 4 and 5 did not indicate total silver concentration but rather claimed to contain colloidal silver. For colloidal silver dietary supplements and spray disinfectants, discrepancies between claimed and measured values for both concentration and form of silver have been previously reported (Cascio et al., 2015; Rogers et al., 2018).

Table 1
Consumer product silver concentration Total Claimed, Total Measured and Soluble.

Product	Total Ag Claimed (mg/l)	Total Ag Measured (mg/l)	Filtrate (soluble Ag) (mg/l)
1	120	18.9 ± 0.9	18.6 ± 0.5
2	500	960.8 ± 28.6	4.9 ± 0.1
3	NR	6.0 ± 1.1	BDL
4	NR	6.1 ± 0.1	BDL
5	NR	8.7 ± 0.7	0.2 ± 0.1

NR Not Reported.
BDL Below Detection Limit.

Variations in pH, as well as the presence of Cl and S may also have an impact on size distribution, interaction with GI fluids, and cellular toxicity assays. The presence of chloride in products 2, 3, 4 and 5 and sulfur in products 1, 2 and 5 may have limited the concentration of Ag + due to the formation of poorly soluble AgCl or Ag_2S. For product 2, the presence of a relatively high concentration of chloride ion compared to the silver found in the soluble fraction suggested the presence of $(AgCl_2)^-$ (Table 1, Table S-1).

3.2. GI simulation and particle size determination

Treatment of the products with SSF was used to approximate the transformation in size and composition of colloidal silver particles during passage through the stomach. Most of the silver in product 1 passed through the 10 kDa filter suggesting that it was ionic or very small nanoparticles <14 nm. The TEM for this sample also showed larger particles (range, 30–200 nm) and very small particles (mean, 2.3 nm). NTA and DLS showed the presence of larger silver particles or particle agglomerates, but due to technical constraints did not show the presence of the smaller particles. TEMs were recorded for product 2 after treatment with SSF, but due to technical issues were not measured for the other products.

Hydrodynamic diameter measurements for both NTA and DLS for product 1 were similar to each other (Table 2). Although the standard deviations (SD) for the NTA measurements were quite large, the mode peak was sharp (Fig. 1, DDI water) indicative of a significant number of particles with a hydrodynamic diameter around 107 nm. Incubation of product 1 with SSF resulted in a significant increase in hydrodynamic

Table 2
Hydrodynamic diameter, primary particle size for selected products before and after treatment with Synthetic Stomach Fluid (SSF).

	Hydrodynamic Diameter (nm)			TEM Particle Diameter (nm)	
Product	NTA Mean	LS_Z-AVG (nm)	PDI	P-1	P-2
1	184 ± 125	166 ± 31	0.43	0.3	30–200
1+ SSF	32 ± 57	180 ± 29	0.33	NM	NM
2	77 ± 38	7 ± 0.6	0.48	0.5	20–40
2+ SSF	278 ± 120	715 ± 65	0.23	5.0	0–50
3	199 ± 209	245 ± 11	0.29	5.5	15–30
3 + SsSF	32 ± 180	ND	ND	NM	NM
4	22 ± 177	220 ± 5.8	0.34	5.2	15–30
4 + SSF	3 ± 48	ND	ND	NM	NM
5	200 ± 72	421 ± 40	0.43	NO	20–50
5 + SSF	311 ± 130	ND	ND	NM	NM

ND Not Determined DLS measurement was not successful.
NM Not Measured.
NO Not Observed.
P-1, P2, Particle size range.

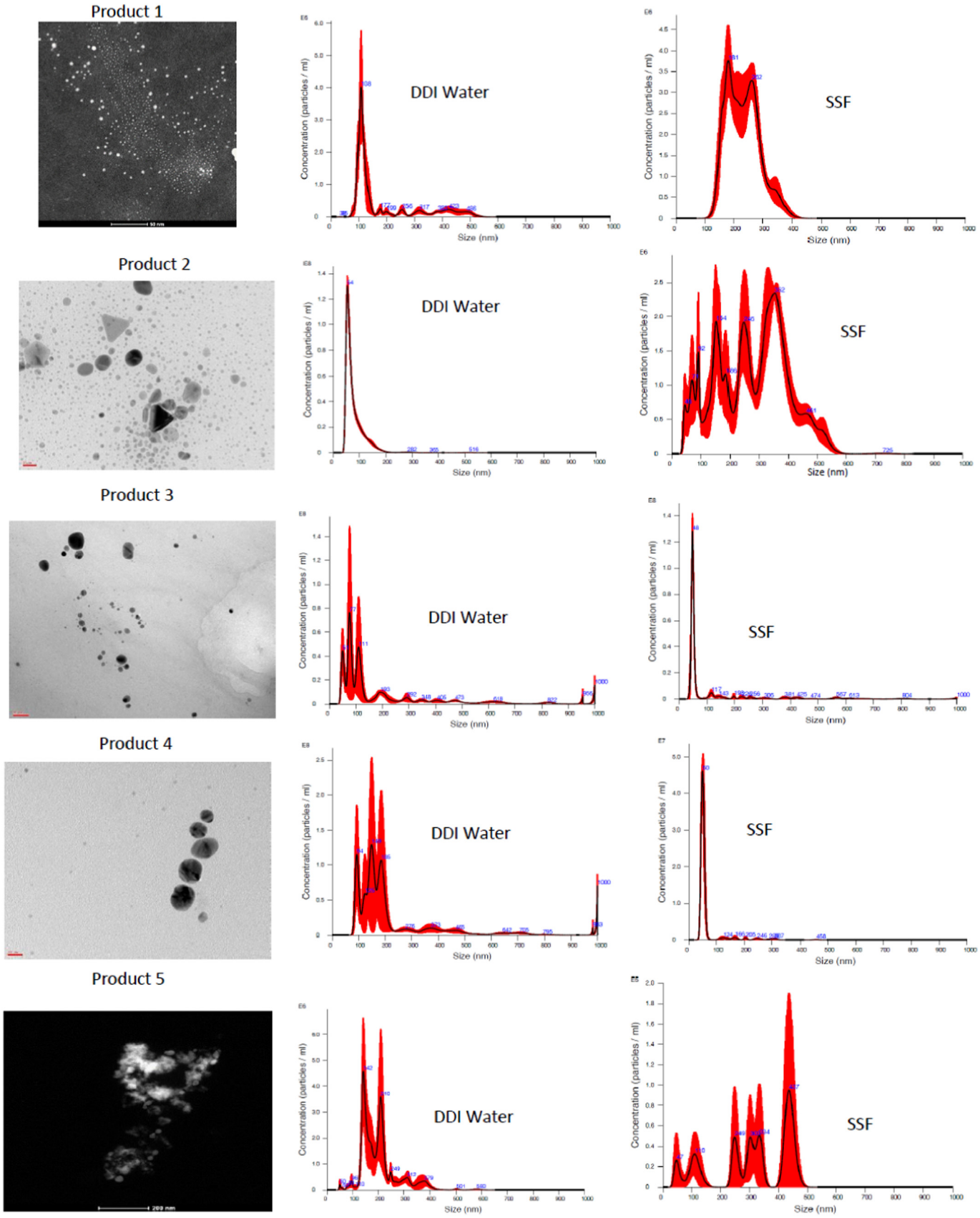

Fig. 1. Particle Size Distribution by TEM and NTA. Products 1–5 TEM images for non-fractionated (as received) products (size bars as noted on images, Product 1, 50 nm; product 2, 20 nm; product 3, 20 nm; product 4, 20 nm; product 5, 200 nm). NTA hydrodynamic diameter distributions for products in DI water or SSF (after 60 min) (black line averages, red line SD for 5 runs). (For interpretation of the references to color in this figure legend, the reader is referred to the web version of this article.)

diameter measured by both the NTA and DLS possibly suggesting the agglomeration of these particles (Table 2). For NTA, the analysis tracing showed at least two particle populations between 200 and 300 nm (Fig. 1, SSF).

Product 2 showed a total measured silver value that was almost double its claimed value (Table 1). This product was largely particulate in nature based on ultrafiltration. TEM analysis showed notable triangular silver nanostructures along with a distribution of particle sizes ranging from about 4 to 40 nm (Fig. 1). Incubation of product 2 with SSF resulted in a small increase in observed particles by TEM. There was, however, a significant increase in average particle hydrodynamic diameter with DLS, more so than with NTA (Table 2). After treatment with SSF, the NTA particle count analysis showed the addition of 4 main peaks extending from 100 to 400 nm (Fig. 1, SSF). Elemental analysis after treatment with SSF also showed a close association of Cl with the agglomerated particles (Fig. S-1). Incubation with simulated GI fluids has been shown to result in agglomeration of commercial and laboratory synthesized AgNPs with the formation of bridging AgCl structures (Walczak et al. 2012; Rogers et al., 2012).

The measured total silver concentrations for products 3 and 4 were about 6 mg/l (Table 1). The silver content for both products was also associated with the particulate fraction and both showing smaller and larger AgNPs (Table 2). Upon addition of SSF, both products showed the formation of large agglomerates beyond the reportable range for DLS (listed as ND in Table 2). For each of these samples the NTA analysis appeared to be consolidated from a polydispersed distribution of larger particles to a more monodispersed distribution of smaller particles (Fig. 1, compare DDI water to SSF). Given the decrease in the total number of particles measured by NTA (data not shown), we suspect that very large agglomerates precipitated out of the measurement window for the NTA sample cell.

For product 5, TEM showed a distribution of particles ranging from 20 to 50 nm while the NTA and DLS showed hydrodynamic diameters for larger particle agglomerates ranging in size from 200 to 400 nm. Addition of SSF resulted in an increase in average hydrodynamic diameter by NTA with six particle number population peaks extending from 50 to 500 nm (Fig. 1, compare DDI water with SSF).

3.3. Cell viability upon exposure to colloidal silver products

The viability of the rat IEC-6 cells was determined as a function of silver nitrate concentration, based on silver ion mass (Fig. 2). In addition to positive (Triton-X 100) and negative (media only) controls, cells were exposed to Ag^+ at concentrations from 0.1 to 5.0 μg/ml resulting in a significant decrease in cell viability at concentrations between 1.0 and 5.0 μg/ml Ag^+ (Fig. 2). A similar experiment was performed with the rat IEC6 cells using 20 nm AgNPs stabilized with PVP where cells were exposed to these nanoparticles at concentrations between 1.0 and 500 μg/ml. Significant toxicity was observed at AgNP concentrations between 100 and 500 μg/ml (Fig. 2).

IEC-6 cells were incubated with colloidal silver spray products at 1:5, 1:10, and 1:20 dilutions for 24 h (Fig. 2). To better approximate user experience including unknown matrix contributions, measured silver in the products and filtrate (soluble) fractions were used as supplied and not normalized for total silver. This approach also included spray products not intended for direct ingestion. The use of spray products near the face, however, has been shown to result in inhalable aerosols at <1 m from the pump spray release (Park et al., 2017). Ingestion may result from inhaled AgNPs contacting the conducting airways which are lined with cilia or the spray contacting the mouth and throat structures may be carried directly to the esophagus in the saliva and swallowed. The cilia may move the particles up the respiratory tract to the pharynx, where the particles are swallowed into the GI tract.

The addition of product 1 to the cell assay resulted in cellular toxicity at the 1:5 dilution (total silver 3.8 μg/ml). The soluble (filtrate) fraction also caused a loss in cell viability at a similar concentration (Fig. 2). Dilution of product 1 and its filtrate to 1:10 and 1:20 alleviated the cytotoxic effect. Because the silver content of this product was mostly soluble, the cellular toxicity is attributed to soluble Ag or possibly very small nanoparticles <3 nm. Product 2 showed the highest total silver concentration for the products tested. The silver was primarily particulate, and the unfractionated product resulted in a significant cellular response at all three dilutions (192, 96, 48 μg/ml) (Fig. 2). The soluble fraction contained only a small percentage of the total silver (1.0 μg/ml at the 1:5 dilution). Since the silver ion dose response did not show a cellular response at this concentration, we attribute the decrease in cell viability to the AgNPs in the product (Fig. 2). It is not clear as to why the dilutions of commercial silver particles and filtrates for products 1 and 2 showed variability values higher than the control samples. Although the cells were washed prior to MTS loading and measurement resolving any colorimetric interference problems, low concentrations of ionic silver or AgNPs may have an indirect effect on the assay.

Product 3 showed the lowest total silver concentration of the products tested. In addition, very little silver (below detection limits for

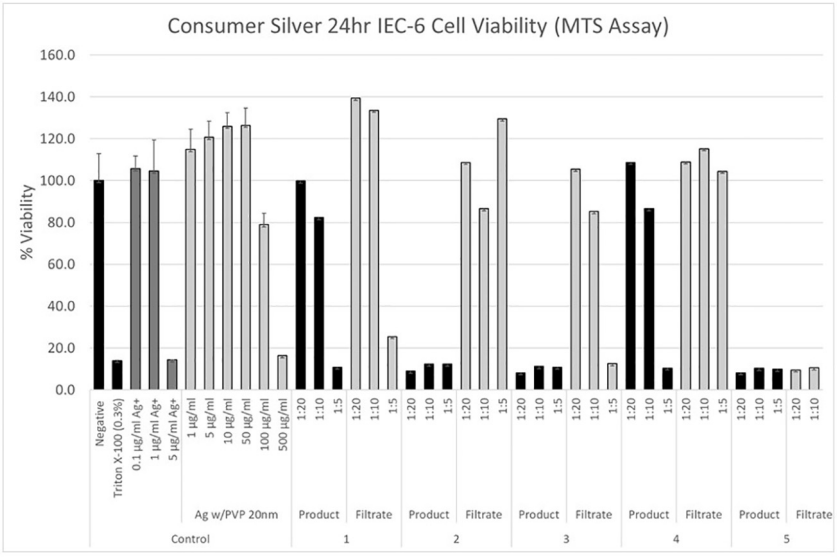

Fig. 2. Cytotoxicity (cell viability) Dose Response for Colloidal Silver Products Using Rat IEC-6 cells. Negative controls (assay media), positive control (0.3% Triton-X-100), silver ion (AgNO3), AgNPs (20 nm pvp-stabilized), products 1–5, filtrates 1–5 (diluted 1:5, 1:10, 1:20 in cell assay media). Mean ± SD.

ICP-OES, 0.1 μg/ml) was present in the soluble fraction. Because neither the soluble fraction nor the unfractionated (mostly particulate silver) product contained sufficient silver to cause a cellular response even at the highest concentration, we attributed the observed toxicity for product 3 to non-silver matrix components (Fig. 2). Although it is not completely clear why the soluble fraction at the lower concentrations (1:10, 1:20) did not also result in greater cellular toxicity, the non-silver matrix components may have been particulate or micellular in nature and were separated by ultrafiltration. Product 4 behaved similarly to product 3; however, in this product, the lower concentrations (1:10, 1:20) of the non-fractionated product did not show the same extent of cellular toxicity.

For product 5, all dilutions of both unfractionated and the soluble fraction resulted in significant cellular responses. This is notable because the lowest concentrations of this product and its soluble fraction did not have enough silver (soluble or particulate) to have resulted in the observed cellular response. Again, these results suggested that matrix components resulted in the cellular response (Table 3).

Several publications have reported on the potential interference of nanoparticles with cellular viability assays (Holder et al., 2012; Monteiro-Riviere et al., 2009; Petersen et al., 2014). In viability assays such the MTS assay, the potential interference may result in a measurement of an artifactual increased or decreased viability. Increased viability may result from the nanoparticle absorbing light at same wavelength as the formazan product or the nanoparticle itself also generates formazan from MTS. Decreased viability may result if the nanoparticle adsorbs formazan (Holder et al., 2012). In the present study, the viability measurement of the cells exposed to AgNPs coated with PVP at doses of 1–50 μg/ml and several of the filtrates of Products 1–4 exceeded the negative control values (10 to 40% higher). This suggested that some unknown factor in addition to the cell's dehydrogenases and reductases reduced the tetrazolium salt MTS to its formazan and colored product. It is not clear why more diluted concentrations of the filtrate of Product 1 results in a higher viability relative to negative control viability results. Alternatively, an unknown component in the filtrate absorbed light at the same wavelength as the formazan product or generated it from MTS. It should be noted that the cells were rinsed with media after the 24-h exposure and before addition of the MTS. This factor may either be absorbed into the cells or could not be removed by the wash.

3.4. GI simulation effect on cellular response to colloidal silver products

The colloidal silver suspensions were exposed to 3 simulated GI fluids (1 gastric fluid and 2 intestinal fluids) prior to the IEC-6 cell assay. This GI simulation assay was similar to that reported by Henson et al. (2019) and involved isolating the suspension particles along with any protein aggregates after each incubation by ultracentrifugation and resuspension. Because the silver in product 1 is primarily soluble and this GI simulation with ultracentrifugation isolates particles, it is not surprising that the 1:5 dilution (highest concentration) did not result in a cell assay response (Fig. 3). For product 2, the GI simulation did not prevent the colloid silver particles from causing a cellular response (Fig. 3). Previously published results have shown that although AgNPs are transformed by exposure to GI fluids, particles are still present and may interact with the intestinal surfaces (Mwilu et al., 2013; Walczak et al., 2012). For product 3, as compared to the AgNP dose response, the amount of particulate silver at the highest dose level would not have been sufficient to result in the observed cellular response. However, non-silver product matrix particulates which appeared to cause the cytotoxic response were not affected by the simulated GI exposure. Again, the response of product 4 was similar to product 3 with a smaller cellular response (Fig. 3). Neither the concentration of particulate silver nor soluble silver in product 5 was sufficient to result in the cellular response. In contrast to products 3 and 4, cytotoxic non-silver matrix components for product 5 did not appear to be carried over in the centrifugation pellet fraction indicating that they were soluble.

Table 3
Suggested cause for cellular response.

Product	Soluble Ag Sufficient to Cause Cell Response (mg/l after 1:5)	Particulate Ag Sufficient to Cause Cell Response (mg/l after 1:5)	Unexplained Response Contribution from Product Matrix (mg/l after 1:5)
1	Yes (3.7)	No (1.6)	No
2	No (1.0)	Yes (191)	No
3	No (BDL)	No (1.2)	Yes[a]
4	No (BDL)	No (1.2)	Yes[a]
5	No (BDL)	No (4.3)	Yes[b]

BDL Below Detection Limit.
Matrix additive reported on the product labels.
[a] Essential Oils (non-specified).
[b] Ethanol, Olive Leaf Extract, Hydrogen Peroxide.

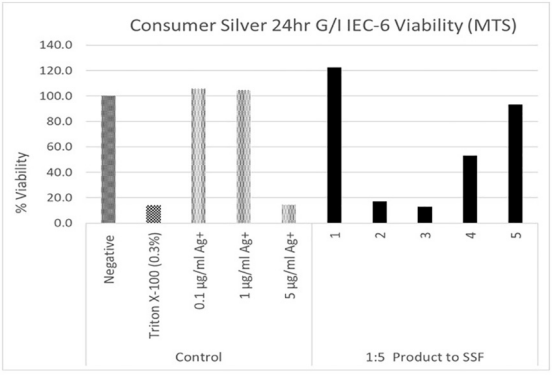

Fig. 3. IEC-6 Cell Viability for Isolated Colloidal Particles Treated with Simulated GI Fluids. Negative controls (assay media), positive control (Triton-X-100), AgNPs (20 nm pvp-stabilized treated with GI fluids). Colloidal products were diluted 1:5 into cell assay media prior to GI fluid assay (+/- SD, n=12).

3.5. Potential for human exposure

These five products show varied potentials for exposure in terms of recommended doses, use frequencies, routes of exposure and forms of silver. For products 1 and 2, we suspect that when applying a pump spray to the mouth with variable distance, inhalation, etc., that a high percentage of the aerosol will impact the mouth and throat surfaces prior to the trachea and will be carried into the esophagus with the expected saliva emission. The stomach/intestinal dilution will depend on the volume of liquid present. For products 3, 4, and 5, the amount of aerosol making its way to the GI tract could be much smaller than the 1:5 dilution, however, inhalation in confined spaces such as shower stalls or closets for an extended use periods such as for occupational applications, could result in higher exposures.

Other factors that may influence exposure include adherence to dilution instructions, intentional or unintentional misuses and for external surface disinfectant spray products, room size, ventilation and proximity to the nose and mouth from the spray release. All of the products were supplied with pump spray devices which typically emit aerosols that are deposited directly or quickly drop on to surfaces (Quadros and Marr, 2010; Park et al., 2017); however, there is also considerable uncertainty as to the potential inhalation exposure of the products used for this study. For aerosol products intended for internal use, distributions of aerosol droplets in the mouth, throat, nasal cavity and deeper into the lungs have not been widely investigated (Rogers et al., 2018).

Based on rodent toxicity studies with endpoints such as weight loss, hypoactivity, altered neurotransmitter levels, altered liver enzymes and argyria, a Tolerable Daily Intake level of 2.5 μg/kg-bw/d with a safety

margin of 5× has been reported by Hadrup and Lam (2014). For a 70 kg person, this translates to ingesting 175 μg/d silver. Product 2 showed the highest concentration of total silver (mostly in particulate form) and given its instructions for a relatively high dose, showed the greatest potential for exposure (Table S-2). Given the EPA Reference dose (RfD) of 350 μg/day (for a 70 kg person), the recommended dose of 961 μg silver for product 2 taken daily "may put a consumer at risk of argyria" (Fung and Bowen, 1996; US Environmental Protection Agency, 1991). This recommended daily dose which exceeds the EPA reference dose may additionally result in toxic effects.

4. Summary

Five commercial colloidal silver spray products that were advertised as dietary supplements, "immune boosters", or surface spray disinfectants were characterized with respect to total silver and soluble silver. The components of these suspensions which contributed to cellular toxicity and may contribute to risk included soluble silver, particulate silver or non-silver matrix components. In addition, mis-labeling of products may lead to very low or significantly high exposures when following instructions for use. Three of the products did not report silver concentrations, while measured total silver concentrations for two of the products were either significantly higher or lower than claimed. Similar discrepancies between claimed and measured levels of total silver have been previously reported for colloidal silver used in a variety of products (Cascio et al., 2015; Rogers et al., 2018). Considering explicit warnings for use of colloidal silver present on websites for the Mayo Clinic, Harvard Medical School and National Center for Complementary and Integrative Health as well as the increasing popularity, increasing number of products and lack of oversight, product mislabeling resulting in higher than expected silver exposure may be a concern. For example, following the dosing instructions for one of the mislabeled products (product 2) would result in a daily dose of silver that is nearly 3× the EPA Oral RfD for a 70 kg individual and exceeds the Tolerable Daily Dose by 5× for adults. In addition to daily dose limits, it has been shown that long-term (months to years) intake of colloidal silver on the order of 100–1000 μg/day can cause argyria (Fung and Bowen, 1996; US Environmental Protection Agency, 1991; Hadrup and Lam, 2014).

The colloidal silver products were further characterized for particle size distribution and particle hydrodynamic diameter both before and after incubation with SSF. As measured by TEM, there appeared to be two silver size distributions in the original products 1–4. The smaller size particle populations ranged in size from 2.3–15 nm while the larger population ranged from 15 to 50 nm. Hydrodynamic diameters measured by NTA and DLS showed larger agglomerates ranging from 50 to 400 nm. Due, in part, to methodological limitations and agglomeration dynamics in suspension, NTA and DLS did not detect the smaller particles. Upon incubation with SSF, in most cases, the AgNPs further agglomerated in suspension. It was also observed that AgCl formation was associated with the AgNP agglomerates in product 2 after incubation with SSF. AgCl formation on AgNP surfaces after incubation with SSF has also been previously reported (Rogers et al., 2012).

Cytotoxicity for each of the products and their soluble fractions was assessed using the rat intestinal cell model. The dose responses for silver ion and particles indicated that the cytotoxic concentrations for ion (between 1 and 5 μg/ml) were lower than for commercially-sourced 20 nm AgNPs (between 100 and 500 μg/ml). By comparing the dose response of the products to those of silver ions and particles, where possible we attributed cellular cytotoxicity in the products to soluble or particulate silver. We also observed cytotoxicity that we attributed to the non-silver matrix constituents when concentrations of either ion or particulate were insufficient to cause the observed cytotoxicity. This result was not unexpected given the variety of nominally reported additives such as essential oils, plant extracts and hydrogen peroxide.

Disclaimer

This work has been primarily funded by the U.S. Environmental Protection Agency and to a lesser extent is part of interagency agreements between the U.S. Environmental Protection Agency (EPA) and the U.S. Consumer Product Safety Commission (CPSC) (EPA-IA-RW-61-92,317,001-0) and NIOSH and CPSC (CPSC-I-10-006). This work has been subjected to EPA administrative review and approved for publication. The findings and conclusions in this paper are those of the authors and do not necessarily represent the views of the CPSC or NIOSH. Mention of trade names or commercial products does not constitute endorsement or recommendation for use, nor does it imply that alternative products are unavailable or unable to be substituted after appropriate evaluation.

CRediT authorship contribution statement

Kim R. Rogers: Conceptualization, Formal analysis, Resources, Writing - original draft, Writing - review & editing, Supervision, Project administration, Funding acquisition.**Taylor E. Henson:**Methodology, Validation, Formal analysis, Investigation.**Jana Navratilova:**Methodology, Validation, Formal analysis, Investigation.**Mark Surette:**Methodology, Validation, Formal analysis, Investigation.**Michael F. Hughes:** Conceptualization, Formal analysis, Writing - review & editing, Supervision.**Karen D. Bradham:**Supervision, Project administration, Funding acquisition.**Aleksandr B. Stefaniak:**Conceptualization, Supervision, Project administration.**Alycia K. Knepp:**Methodology, Validation, Formal analysis, Investigation.**Lauren Bowers:**Methodology, Validation, Formal analysis, Investigation.

Declaration of competing interest

The authors declare that they have no known competing financial interests or personal relationships that could have appeared to influence the work reported in this paper.

Acknowledgements

This project was supported in part by an appointment to the Internship/Research Participation Program at the Office of Research and Development, U.S. Environmental Protection Agency, administered by the Oak Ridge Institute for Science and Education through an interagency agreement between the U.S. Department of Energy and EPA.

Appendix A. Supplementary data

Supplementary data to this article can be found online at https://doi.org/10.1016/j.scitotenv.2020.138611.

References

Bohmert, L., Girod, M., Hansen, U., Maul, R., Knappe, P., Niemann, B., Weidner, S.M., Thunemann, A.F., Lampen, A., 2014. Analytically monitored digestion of silver nanoparticles and their toxicity on human intestinal cells. Nanotoxicology 8, 631–642.

Cascio, C., Geiss, O., Franchini, F., Ojea-Jimenez, I., Rossi, F., Gilliland, D., Calzolai, L., 2015. Detection, quantification and derivation of number size distribution of silver nanoparticles in antimicrobial consumer products. J. Anal. Spectrom. 30, 1255–1265.

Danaei, M., Dehghankhold, M., Ataei, S., Hasanzadeh Davarani, F., Javanmard, R., Dokhani, A., Khorasani, S., Mozafari, M.R., 2018. Impact of particle size and polydispersity index on the clinical applications of lipidic nanocarrier systems. Pharmaceutics, 57–74 https://doi.org/10.3390/Pharmaceutics10020057.

FDA, 1999. Advisory for colloidal silver over-the-counter drug products containing colloidal silver ingredients or silver salts: final rule. https://www.govinfo.gov/content/pkg/FR-1999-08-17/pdf/99-21253.pdf, Accessed date: 30 March 2020.

Fung, M.C., Bowen, D.L., 1996. Silver products for medical indications: risk-benefit assessment. Clin. Toxicol. 34, 119–126.

Hadrup, N., Lam, H.R., 2014. Oral toxicity of silver ions, silver nanoparticles and colloidal silver. Reg. Toxicol. Pharmacol. 68, 1–7.

Henson, T.E., Navratilova, J., Tennant, A.H., Bradham, K.D., Rogers, K.R., Hughes, M.F., 2019. In vitro intestinal toxicity of copper oxide nanoparticles in rat and human cell models. Nanotoxicology 13, 795–811. https://doi.org/10.1080/1745390.2019.1578428.

Holder, A.L., Goth-Goldstein, R., Lucas, D., Koshland, C.P., 2012. Particle-induced artifacts in the MTT and LDH viability assays. Chem. Res. Toxicol. 25, 1885–1892.
Kastner, C., Lichtenstein, D., Lampen, A., Thunemann, A.F., 2017. Monitoring the fate of small silver nsnoparticles during artificial digestion. Colloidal and Surfaces A; Physicochem. Eng. Aspects. 526, 76–81.
Kelly, M.E., Schoof, R.A., Ruby, M.V., 2002. Assessing Oral Bioavailability of Metals in Soil. Battelle Press, Columbus.
Kim, J.J., Konkel, K., McCulley, L., Diak, I.-L., 2019. Cases of argyria associated with colloidal silver use. Annals Pharmacotherapy 53, 867–870.
Kwon, H.B., Lee, J.H., Lee, S.O., Lee, A.Y., Choi, J.S., Ahn, Y.S., 2009. A case of argyria following colloidal silver ingestion. Ann. Dermatol. 21, 308–310.
Lim, J.-H., Bairi, V.G., Linder, S.W., Fong, A., 2019. Detection and characterization of silver nanostructures in consumer products. J Nanoscience Nanotechnol 19, 8078–8087.
MacCuspie, R.I., Rogers, K., Patra, M., Suo, Z., Allen, A.J., Martina, M.N., Hackley, V.A., 2011. Challenges for physical characterization of silver nanoparticles under pristine and environmentally relevant conditions. J. Environ. Monit. 13, 1212–1226.
Mayo Clinic, d. https://www.mayoclinic.org/healthy-lifestyle/consumer-health/expert-answers/colloidal-silver/faq-20058061, Accessed date: 30 March 2020.
McCracken, C., Zane, A., Knight, D.A., Dutta, P.K., Waldman, W.J., 2013. Minimal intestinal epithelial cell toxicity in response to short- and long-term food-relevant inorganic nanoparticle exposure. Chem. Res. Toxicol. 26, 1514–1525.
Miethling-Graff, R., Rumpker, R., Richter, M., Varano-Braga, T., Kjeldsen, F., Brewer, J., Hoyland, J., Rubahn, H.-G., Erdmann, H., 2014. Exposure to silver nanoparticles induces size-and dose-dependent oxidative stress and cytotoxicity in human colon carcinoma cells. Toxicol. in Vitro 28, 1280–1289.
Monteiro-Riviere, N.A., Inman, A.O., Zhang, L.W., 2009. Limitations and relative utility of screening assays to assess engineered nanoparticle toxicity in a human cell line. Toxicol. Appl. Pharmacol. 234, 222–235.
Munger, M.A., Radwanski, P., Hadlock, G.C., Stoddard, G., Shaaban, A., Falconer, J., Grainger, D.W., Deering-Rice, C.E., 2014. In vivo human time-exposure study of orally dosed commercial silver nanoparticles. Nanomedicine: NBM 10, 1–9.
Mwilu, S.K., El Badawy, A.M., Bradham, K., Nelson, C., Thomas, D., Scheckel, K.G., Tolaymat, T., Ma, L., Rogers, K.R., 2013. Changes in silver nanoparticles exposure to human synthetic stomach fluid: effects of particle size and surface chemistry. Sci. Total Environ. 447, 90–98.
Park, J., Ham, S., Jang, M., Lee, J., Kim, S., Kim, S., Lee, K., Park, D., Kwon, J., Kim, H., Kim, P., Choi, K., Yoon, C., 2017. Spacial-temporal dispersion of aerosolized nanoparticles during the use of consumer spray products and estimates of inhalation exposure. Environ. Sci. Technol. 51, 7624–7638.
Petersen, E.J., Henry, T.B., Zhao, J., MacCuspie, R.I., Kirschling, T.L., Dobrovolskaia, M.A., Hackley, V., Xing, B., White, J.C., 2014. Identification and avoidance of potential artifacts and misinterpretations in nanomaterial ecotoxicity measurements. Environ. Sci. Technol. 48, 4226–4246.
Quadros, M.E., Marr, L.C., 2010. Environmental and human health risks of aerosolized silver nanoparticles. J. Air Waste Manage. Assoc. 60, 770–781.
Ramos, K., Ramos, L., Camara, C., Gomez-Gomez, M.M., 2014. Characterization and quantification of silver nanoparticles in nutraceuticals and beverages by asymmetric flow field flow fractionation coupled with inductively coupled plasma mass spectrometry. J. Chromatogr. A 1371, 227–236.
Reed, R.B., Faust, J.J., Yang, Y., Doudrick, D.G., Hristovski, K., Westerhoff, P., 2014. Characterization of nanomaterials in metal colloid-containing dietary supplement drinks and assessment of their potential interactions after ingestion. ACS Sustain. Chem. Eng. 2, 1616–1624.
Rogers, K.R., Bradham, K., Tolaymat, T., Thomas, G.J., Hartmann, T., Ma, L., Williams, A., 2012. Alterations in physical state of silver exposed to synthetic stomach fluid. Sci. Total Environ. 420, 334–339.
Rogers, K.R., Navratilova, J., Stefaniak, A., Bowers, L., Knepp, A.K., Al-Abed, S.R., Potter, P., Gitipour, A., Radwan, I., Nelson, C., Bradham, K., 2018. Characterization of engineered nanoparticles in commercially available spray disinfectant products advertised to contain colloidal silver. Sci. Total Environ. 619–620, 1375–1384.
Saluja, S.S., Bowen, A.R., Hull, C.M., 2015. Case report: Argyria – a case of blue-gray skin. Journal of Drugs in Dermatology 14, 760–761.
US Environmental Protection Agency, 1991. Reference Dose for Chronic Oral Exposure of Silver. Chemical screening and risk assessment division, Washington, DC CASRN 7440-22-4.
Van Koetsem, F., Verstraete, S., Wallaert, E., Verbeken, K., Van der Meeren, P., Rinklebe, J., Laing, G.D., 2017. Use of filtration techniques to study environmental fate of engineered metallic nanoparticles: factors affecting filter performance. J. Hazard. Mater. 322, 105–117.
Walczak, A.P., Fokkink, R., Peters, R., Tromp, P., Herrera Rivera, Z.E., Rietjens, I., Hendriksen, P.J.M., 2012. Behavior of silver nanoparticles in an in vitro human gastrointestinal digestion model. Nanotoxicology 7. https://doi.org/10.3109/17435390.2012.72632 1898-1210.
Wu, W., Zhang, R., McClements, D.J., Chefetz, B., Polubesova, T., Xing, B., 2018. Transformation and speciation analysis of silver nanoparticles of dietary supplement in simulated human gastrointestinal tract. Environ. Sci. Technol. 52, 8792–8800.